Article

Estimation of the Constituent Properties of Red Delicious Apples Using a Hybrid of Artificial Neural Networks and Artificial Bee Colony Algorithm

Yousef Abbaspour-Gilandeh [1,*] **, Sajad Sabzi** [1]**, Brahim Benmouna** [2]**, Ginés García-Mateos** [2,*]**, José Luis Hernández-Hernández** [3] **and José Miguel Molina-Martínez** [4]

[1] Department of Biosystems Engineering, College of Agriculture, University of Mohaghegh Ardabili, Ardabil 56199-11367, Iran; s.sabzi@uma.ac.ir
[2] Computer Science and Systems Department, University of Murcia, 30100 Murcia, Spain; benmouna_brahim@yahoo.fr
[3] Division of Research and Graduate Studies, TecNM/Technological Institute of Chilpancingo, Chilpancingo, Guerrero 39070, Mexico; joseluis.hernandez@itchilpancingo.edu.mx
[4] Food Engineering and Agricultural Equipment Department, Technical University of Cartagena, 30203 Cartagena, Spain; josem.molina@upct.es
*   Correspondence: abbaspour@uma.ac.ir (Y.A.-G.); ginesgm@um.es (G.G.-M.); Tel.: +34-868-888-530 (G.G.-M.)

check for updates

Abstract: Non-destructive estimation of the constituent properties of fruits and vegetables has led to a dramatic change in the agriculture and food industry, allowing accurate and efficient sorting of the products based on their internal properties. Therefore, the present study utilized visible (VIS) and near-infrared (NIR) spectroscopy data in the range from 200 to 1100 nm for the estimation of several properties of Red Delicious apples, namely Brix minus acid (BrimA), firmness, acidity and starch content, using a hybrid of Artificial Neural Networks and Artificial Bee Colony (ANN–ABC) algorithm. Furthermore, the hybrid Artificial Neural Network–Particle Swarm Optimization (ANN–PSO) algorithm was utilized to select the most effective properties to estimate these characteristics. The results indicated that there are different peaks within this spectral range, and the spectral range for each peak gives different results. To ensure the stability of the proposed method, 1000 replications were performed for each estimate. The highest coefficients of determination, R^2, for estimating the studied properties among the 1000 replicates were 0.898 for BrimA, 0.8 for firmness, 0.825 for acidity and 0.973 for starch content. The selection of the most effective wavelengths for estimating the properties produced five effective wavelengths for BrimA, nine for firmness, seven for acidity and five for starch content. In this case, the best R^2 of the hybrid ANN–ABC among the 1000 iterations were 0.828, 0.738, 0.9 and 0.923, respectively.

Keywords: non-destructive estimation; internal fruit properties; hybrid neural networks; artificial bee colony algorithm; particle swarm optimization algorithm; sorting

---

1. Introduction

The importance of fruit sorting and grading is increasing in the agro-industry and global economy. The classification of fruits based on their internal and external qualitative features enables intelligent management at the different stages of fruit distribution and processing [1]. The appearance, color, size and absence of defects on fruits are some of the most important qualitative characteristics based on external fruit properties [2]. On the other hand, the most important internal or constituent properties, which attract buyers, include Soluble Solids Content (SSC), Titratable Acidity (TA) and the ratio of Soluble Solids Content to Titratable Acidity [3–6].

Conventional methods for measuring internal properties of fruits are a kind of destructive method, since the fruits are destroyed in the process. In the last decade, however, non-destructive methods have received more interest due to permitting individual measurement and analysis of fruits, reducing waste and allowing repeated measurements at the same conditions for different times [7]. Some of these non-destructive methods include near-infrared spectroscopy (NIRS) [7–11], mid-infrared spectroscopy (MIRS) [10,12], hyperspectral imaging (HSI) [10,13], ultraviolet–visible spectroscopy (UV–vis) [14], Raman spectroscopy [10] and the Proton Transfer Reaction Mass spectrometry (PTR–MS) [15,16]. Among these non-destructive methods, NIRS is the most widely used for quality control in food and agricultural industries [7,17].

For example, in the work by Moscetti et al. [18], hailstorm damage was detected on olive using NIRS. For this purpose, 744 olives were used and the spectrums in the range from 1100 to 2300 nm were obtained with a Luminar 5030 Acousto-Optic Tunable Filter Near-Infrared (AOTF–NIR) Miniature "Hand-held" Analyzer (Brimrose Corp., Baltimore, MD, USA). A genetic algorithm was used for selecting the input properties for three classifiers: Linear Discriminant Analysis (LDA), Quadratic Discriminant Analysis (QDA) and k-nearest neighbor (KNN). The wavelengths selected by the genetic algorithm were 1320, 1460, 1650, 1920, 2080, 2200 and 2220 nm. The determination of the fruit ripening degree is another application of the spectroscopy method. In this regard, Neto et al. [19] conducted a study to determine the ripening stage of mango fruits using electrical impedance spectroscopy. This technique is based on changes in the bulk resistance depending on fruit ripening due to the changes in the fluid content of fruit fibers. The results indicated a strong correlation between mechanical measurements and electrical parameters. Therefore, it is possible to measure the degree of fruit ripening using this non-destructive method.

Another interesting application is the non-destructive estimation of the constituent properties of the fruits. Bizzani et al. [20] developed a method to estimate the firmness, skin thickness and total pectin content. They used Partial Least Square Regression (PLSR) models of data of Time Domain Nuclear Magnetic Resonance (TD–NMR) spectroscopy, NIRS and MIRS to predict these properties in fresh Valencia oranges. The results indicated that NIRS and MIRS produced the best PLSR models for predicting orange firmness, with Pearson Correlation Coefficients (PCC) of 0.92 and 0.84, respectively. The PLSR model relating to the TD–NMR for predicting the orange peel thickness achieved a PCC of only 0.72. Finally, the total pectin content was predicted using TD–NMR and NIRS with PCC of 0.76 and 0.70, respectively. In another research, Xie et al. [21] performed the non-destructive estimation of the amounts of titratable acidity, malic acid and citric acid in bayberry using NIRS. For this, 129 samples of bayberry juice were prepared from 14 different cultivars, and nine different regions in China. The studied spectral range was 400 to 1250 nm. The results indicated that the correlation coefficient, R, was 0.896, 0.669 and 0.897 for the prediction of the best model for the titratable acidity, malic acid and citric acid, respectively.

Therefore, these fruit analysis methods based on spectroscopy are gaining interest in the research community around the world because they are fast, non-destructive and can be widely used in sorting based on the internal properties of the fruits. Some aspects that are important to consider are the procedure for applying these methods, and the accuracy of the predicted values using robust estimation methods. Consequently, the present study used a hybrid technique based on Artificial Neural Networks and the Artificial Bee Colony (ANN–ABC) algorithm for the non-destructive estimation of some constituent properties of the fruits. These properties include Brix minus acid (BrimA), firmness, acidity and starch content of Red Delicious apples in the VIS–NIR spectrum. Furthermore, the most effective wavelengths of the spectrum were selected using a hybrid of Artificial Neural Networks and the Particle Swarm Optimization (ANN–PSO) algorithm. Then, the selected wavelengths were used as the input to the hybrid ANN–ABC algorithm to estimate the same constituent properties.

2. Materials and Methods

2.1. Sampling and Collection

Since the most important purpose of the present study was the non-destructive estimation of different constituent properties of Red Delicious apples, the most adequate harvest days were asked to different gardeners of Kermanshah, Iran (34°18′48.87″ N, 47°4′6.92″ E). After determining these harvest dates, four stages were planned for the data collection. In each stage, 16 trees were randomly selected for harvesting. The first stage was 135 days after flowering, and 55 apple samples were harvested at this stage. The second stage was 145 days after flowering, and 53 apple samples were harvested. The third stage was 155 days after flowering, and 56 samples were obtained. Finally, the fourth stage was 165 days after flowering, with 55 samples. During the harvest process, apples with a healthy appearance and medium size were collected, giving an average size in length of 57.47 mm (3.07 mm standard deviation), width 63.01 mm (3.67 mm standard deviation) and height 62.61 mm (3.53 mm standard deviation). The color at the first stage was almost green, and at the fourth stage was mostly red. At each stage after harvesting, the samples were transferred to Shahid Beheshti University for spectral data extraction, and then their mechanical and physicochemical properties were extracted in Karaj Agricultural Engineering Research Institute. The resulting dataset was divided into training and test sets.

2.2. Extracted Spectral Data

The radiation of electromagnetic waves to a material absorbs and reflects certain wavelengths according to the properties of the material. This interaction between radiation and material provides information in spectroscopic studies. In fruits and vegetables, the radiation absorption process is mostly due to C-H, O-H and N-H bonds [7]. Figure 1 shows the configuration of the spectroscopy system used in the present research.
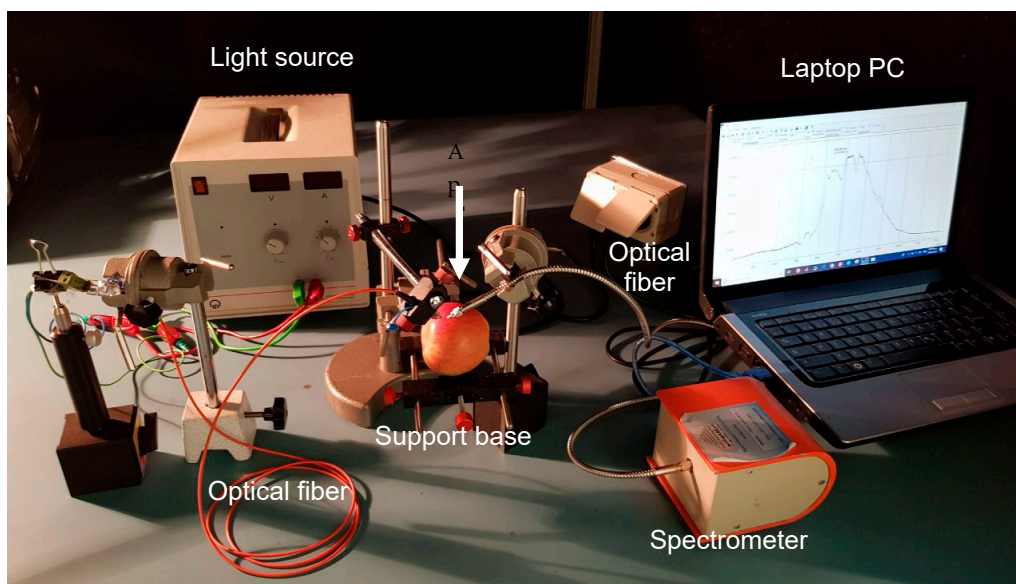

Figure 1. Configuration of the spectroscopy system used in this study.

The spectrometer used in this research was an EPP200NIR model (StellarNet Inc., Tampa, FL, USA) with an indium–gallium–arsenide detector. It has a working range from 200 to 1100 nm and a resolution between 0.1 and 0.4 nm. The reflective mode was the measurement mode used in the study. The spectrometer was connected by a USB2 cable to a laptop PC, equipped with SpectraWiz® software (StellarNet Inc., Tampa, FL, USA) to save the resulting spectra on the computer. The light source was an SLI-CAL model (StellarNet Inc., Tampa, FL, USA) made of 20 W tungsten halogen. A two-strand

optical fiber was used to direct the light beam from the light source to the apple and from the apple to the spectrometer.

Four random points on each apple were used for the analysis, and the average of their spectral data was considered in the study. The exact location of the optical fiber is not important, because the radiation penetrates the apples. The wavelengths from 200 to 400 nm and from 1000 to 1100 nm were eliminated due to the high noise that was observed in these bands; hence, the examined spectral range was 400 nm to 1000 nm. Due to the noise produced by the spectrometer, we eliminated 13 samples from the 55 samples of the first stage, 8 samples from the 53 samples of the second stage, 5 samples from the 56 samples of the third stage and 6 samples from the 55 samples of the fourth stage. Therefore, the number of samples from the first to fourth stages for the analysis were 42, 45, 51 and 49, respectively.

2.3. Reflection and Absorption Spectra

According to Nicolaï et al. [7], the reflection spectra of different fruits such as apples, oranges, nectarines and pears are similar. This means that the occurrence of spectral peaks is similar in the charts of these fruits. As an example, Figure 2 shows the mean reflection spectrum of VIS–NIR light for the 187 apple samples considered, computed using the ParLeS software (IM Publications LLP, Chichester, UK).
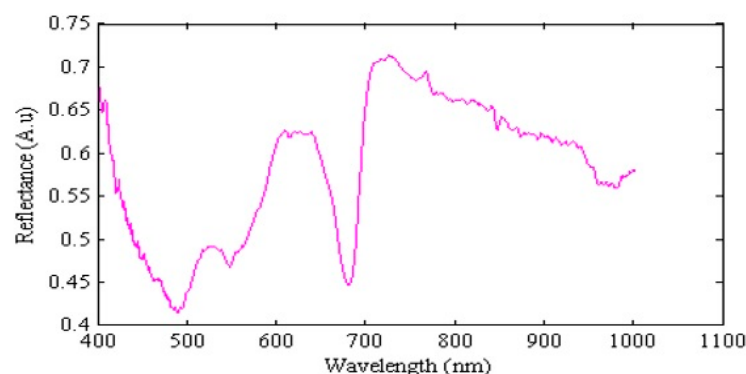

Figure 2. Mean reflection of the visible and near-infrared (VIS–NIR) spectrum for the obtained apple samples.

This software is also able to convert the reflection spectra, R, to the absorption spectra by taking $\log(1/R)$ to reduce the nonlinearity that may exist in the data [22]. Figure 3 shows the mean absorption spectrum of VIS–NIR light for the 187 apple spectra considered. It can be observed that there are different peaks in this spectral range. The peak at 490 nm is attributed to carotenoid absorption; the peaks at 549 and 680 nm are related to chlorophyll A absorption [23,24]; the peaks for 849 and 875 nm are due to the N-H bond; and finally, the peak corresponding to 962 nm wavelength belongs to O-H and C-H bonds [25].
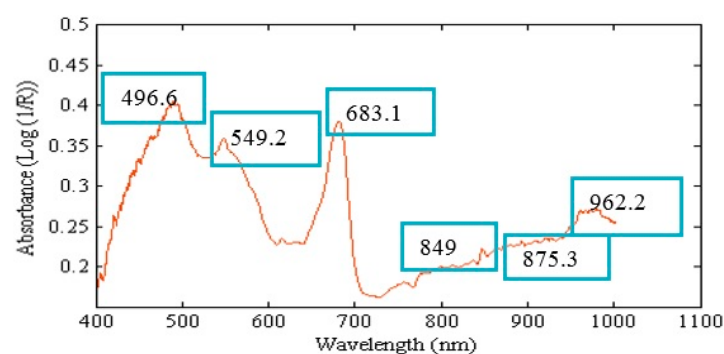

Figure 3. Mean absorption spectrum of VIS–NIR for the obtained apple samples.

2.4. Extraction of the Constituent Properties of the Apples

2.4.1. Measurement of the BrimA Property

BrimA is an abbreviation of Brix minus acids. It was introduced by Jordan et al. [26], as a parameter that is highly related to the sweetness and flavor of the fruits. Using it, sweetness and flavor of the fruits have been estimated by different authors [27]. This parameter is based on Total Soluble Solids (TSS) and Titratable Acidity (TA). TSS is measured as a percentage that indicates the content of soluble sugars with a contribution from the fruit's acids, and TA is generally expressed as a percentage of the predominant acid. Specifically, this index is calculated using the following equation:

$$\text{BrimA} = \text{TSS} - K \times \text{TA} \tag{1}$$

where K is a constant coefficient equal to 5 [28].

2.4.2. Measurement of the Firmness

Apple firmness was measured using a hand-pushed penetrometer. Therefore, a special apple probe was used, consisting of a cylindrical rod attached to the machine, with 11 mm of diameter and 8 mm of height to the marker, for dipping into the apples.

According to the standard recommended procedure [29], the penetrometer was first calibrated, and then each apple was tested on two opposite sides without fruit peel. The mean of these two measurements was stored as the firmness. The numbers were calculated and recorded in terms of force in Newton (N). During the test, it was tried to ensure that the applied force rate was equal in all the samples [29]. For this purpose, the penetrometer was first calibrated and then a part of the fruit peel was removed with a peeler. The tip of the penetrometer was put into the peeled place, and the cylindrical probe was gently dipped into the tissue at a balanced speed. Finally, the amount of applied pressure in N was read from the machine by hand.

2.4.3. Measurement of the Acidity

The acidity of the apple juice was measured using a pH meter of model 8689 AZ Detachable pH Pen (AZ Instrument Corp., Taichung, Taiwan). To obtain the juice, first, the middle part of each apple was peeled to remove the seeds. Then, a slice of the apple was cut and crushed in a mortar, and the juice was extracted from it using a strainer.

2.4.4. Measurement of the Starch Content

Starch is a complex carbohydrate that contains many glucose units linked by a glycosidic bond. To measure starch content in an apple, some juice was extracted as explained in the previous subsection. Then, this juice was dissolved in a mixture of dimethyl sulfoxide and hydrochloric acid. The ratio of dimethyl sulfoxide to hydrochloric acid was 4 to 1. After that, it was centrifuged at 12,000 rpm for 15 min. To prepare the iodine reagent, hydrochloric acid, 0.06 g of potassium iodide and 0.003 g of iodine were dissolved in 100 mL of 0.05 N hydrochloric acid. A mixture of 0.5 mL of iodine reagent (yellow reagent) and 0.5 mL of juice were poured into a small plastic tube and thoroughly mixed. After 15 min, the absorption was read at 600 nm using a spectrophotometer Optizen 2120 UV plus (Mecasys Co. Ltd., Daejeon, Korea). The results were presented in mg/g of fresh weight. Standard glucose solutions were prepared in the next step [30]. Different glucose concentrations from 0 to 100 mg/L were used to prepare these solutions. Then, a scatter plot was drawn relating to the given concentrations and the corresponding absorption values at 600 nm. A linear curve was fit to this scatter plot, obtaining an equation to convert each absorption value into the starch content in mg/L. Finally, starch content in the apples was determined using this equation and the corresponding absorption values. To facilitate its reading, in the experiments, this value is expressed as a percentage of the total weight.

2.5. Hybrid Artificial Neural Networks–Particle Swarm Optimization (ANN–PSO) Algorithm

The hybrid technique of Artificial Neural Networks and Particle Swarm Optimization algorithm (ANN–PSO) was used to select the most effective spectral wavelengths for estimating the predefined constituent properties. PSO is a meta-heuristic algorithm that emulates the mass movements of birds to solve different optimization problems. This algorithm was first proposed by Kennedy and Eberhart [31]. Each possible answer to the problem is considered as a particle. All particles are constantly searching and moving. The motion of each particle depends on three factors: (1) the current position of the particle; (2) the best position that this particle has ever had; and (3) the best position that the whole set of particles have ever had [31]. In our case, the whole extracted wavelengths were first considered as a vector. In the next step, other vectors with different sizes were selected and sent to the ANN using the PSO algorithm.

The multilayer perceptron ANN divides the dataset into three disjoint categories: the first category contains 70% of the samples for training; the second category contains 15% for validation; and the third category contains the remaining 15% for testing. The ANN produces a Mean Square Error (MSE) for each selection of wavelengths, in the estimation of each constituent property. Finally, this MSE of each vector is sent to the PSO optimization algorithm. The vector that produces the least MSE is selected as the set of most effective wavelengths.

Table 1 presents the hyperparameters of the ANN applied to select the most effective wavelengths with the PSO algorithm. The transfer functions, the backpropagation network training functions and the weight/bias-backpropagation learning functions were selected from the Neural Network Toolbox of the MATLAB software (MathWorks, Natick, MA, USA). The designed network has two hidden layers. The hyperbolic tangent sigmoid (*tansig*) is used as the activation function for the hidden layers, the scaled conjugate gradient backpropagation (*trainscg*) is used to train the network and the Hebb weight learning function (*learnhd*) is used to adapt the network.

Table 1. Hyperparameters of the multilayer perceptron ANN used in the Artificial Neural Network–Particle Swarm Optimization (ANN–PSO) algorithm.

Number of Layers	Number of Neurons	Transfer Function	Backpropagation Network Training Function	Backpropagation Weight/Bias Learning Function
2	1st layer: 8 2nd layer: 12	1st layer: *tansig* 2nd layer: *tansig*	*trainscg*	*learnhd*

2.6. Hybrid Artificial Neural Networks–Artificial Bee Colony (ANN–ABC) Algorithm

The hybrid method of Artificial Neural Networks and Artificial Bee Colony algorithm (ANN–ABC) was used to estimate the defined set of constituent properties. The ABC algorithm is inspired by how bees behave in nature. In a beehive, a number of bees are responsible for searching food sources; in the optimization problem, this would mean producing initial responses. After identifying food sources, the bees return to the hive and inform other bees that are called worker bees. Worker bees are sent to these regions to check the amount and quality of the food, and then they return to the hive. This will continue until a food source is identified in large quantities and quality. In the optimization problem, this operation means finding optimal points [32].

The task of the ABC algorithm is to determine the optimal values of the ANN parameters. This network has 5 adjustable parameters: number of layers; number of neurons per layer; transfer function of each layer; backpropagation network training function; and weight/bias-backpropagation learning function. If these parameters have optimal values, the neural network will achieve the highest efficiency.

In the present study, the number of neurons per layer could be at least 0 and at most 25; and the number of layers could be between 1 and 3. The transfer functions, the backpropagation network

training functions and the weight/bias-backpropagation learning functions were again selected from MATLAB Neural Network Toolbox. To this end, the ABC algorithm first considers a vector with the same size as the number of the listed parameters, with between 4 and 8 members. Each member represents a parameter. For instance, the vector $x = \{8, 21, hardlim, poslin, trainbfg, learngd\}$ indicates that the corresponding ANN has 2 hidden layers with 8 and 21 neurons. The hard-limit (*hardlim*) transfer function is used in the first layer, and the positive linear (*poslin*) transfer function is used in the second layer. The BFGS quasi-Newton (*trainbfg*) function is used to train the network, and the gradient descent (*learngd*) weight/bias-backpropagation learning function is used to adapt the network.

The result of each vector transferred to the ANN is measured with the MSE. Finally, the vector with the least MSE is used as the optimal vector of parameters of the multilayer perceptron ANN. Since different ANN were used in the present research to estimate each constituent property, only a sample table of optimal parameters is presented. Table 2 presents these optimal parameters for estimating BrimA property. This network has 3 hidden layers, with 25 neurons in each layer. The hyperbolic tangent sigmoid (*tansig*) is used as the activation function of the hidden layers, the Levenberg–Marquardt backpropagation algorithm (*trainlm*) is used to train the network, and the LVQ1 weight learning function (*learnlv1*) is used to adapt the network.

Table 2. Optimal values of the multilayer perceptron ANN parameters found by the Artificial Bee Colony (ABC) algorithm for the estimation of the Brix minus acid (BrimA) property.

Number of Layers	Number of Neurons	Transfer Function	Backpropagation Network Training Function	Backpropagation Weight/Bias Learning Function
3	1st layer: 25 2nd layer: 25 3rd layer: 25	1st layer: *tansig* 2nd layer: *tansig* 3rd layer: *tansig*	*trainlm*	*learnlv1*

2.7. Predictive Model Evaluation Parameters

The parameters used to evaluate the accuracy of the models for the estimation of the constituent properties using the hybrid ANN–ABC were the Mean Square Error (MSE), the Root Mean Square Error (RMSE), the Mean Absolute Error (MAE) and the coefficient of determination R^2 [33,34]. The formulas to calculate these parameters are as follows:

$$\text{MSE} = \frac{1}{n} \sum_{s=1}^{n} (X_s - Y_s)^2 \tag{2}$$

$$\text{RMSE} = \sqrt{\frac{1}{n} \sum_{s=1}^{n} (X_s - Y_s)^2} \tag{3}$$

$$\text{MAE} = \frac{1}{n} \sum_{s=1}^{n} |X_s - Y_s| \tag{4}$$

$$R^2 = 1 - \left\{ \frac{\sum_{s=1}^{n} (X_s - Y_s)^2}{\sum_{s=1}^{n} (X_s - X_m)^2} \right\} \tag{5}$$

$$X_m = \frac{1}{n} \sum_{s=1}^{n} X_s \tag{6}$$

where n is the number of samples in the test set, X_s is the measured value of the property for the sample s, Y_s is the estimated value of the property for sample s and X_m is the mean of the measured values of the property. Some research works also report the regression coefficient, R, which is simply computed as the square root of R^2.

On the other hand, given a certain accuracy measure (MSE, RMSE, MAE or R^2), since the experiment is repeated many times, it is interesting to report not only the mean value obtained, but also the standard deviation (SD) of this measure. This value indicates the stability of the method in different executions, being the ideal situation an SD near 0. Let us suppose an accuracy measure M, which is repeated m times, producing values M_j for $j = 1, \ldots, m$. The SD of this measure is defined as:

$$SD(M) = \sqrt{\frac{1}{m-1} \sum_{j=1}^{m} \left(M_j - \overline{M}\right)^2}$$

(7)

where $\overline{M}$ is the average of the values of M_j.

3. Results and Discussion

3.1. Estimation of the Constituent Properties Using Spectral Information

As presented in Figure 3, a total of six peak wavelengths were used between 400 and 1000 nm to estimate the constituent properties of Red Delicious apples. In this section, the results for estimating the predefined mechanical and physicochemical properties of the apples related to these peaks in the test data are presented.

3.1.1. Estimation of BrimA

In the estimation of the properties, the hybrid approach ANN–ABC was repeated 1000 times for the estimation of BrimA property, in this case using spectral data around the wavelength 962 nm. Table 3 presents the obtained results in terms of the accuracy evaluation parameters.

Table 3. Mean and standard deviation of the performance evaluation parameters of the hybrid ANN–ABC method in estimating the BrimA property on the spectral data around the wavelength of 962 nm for the 1000 iterations.

Criterion	MSE	RMSE	MAE	R	R^2
Mean	0.0659	0.2529	0.2005	0.8806	0.7775
Standard deviation	0.0242	0.0441	0.0345	0.0450	0.0768

Error measures: Mean Square Error (MSE), Root Mean Square Error (RMSE) and Mean Absolute Error (MAE). Regression coefficient, R, and coefficient of determination, R^2.

The standard deviation of the performance evaluation parameters is acceptable because their values are small, compared to the typical values of this property. Figure 4 shows the regression analysis of the scatter plot between the estimated and the measured values of BrimA of the apples, using a spectral data range around the wavelength of 962 nm in the best training execution. As shown in this figure, the regression coefficient R was 0.948 (coefficient of determination R^2 0.898) for the best execution of the hybrid ANN–ABC method, which can be considered an acceptable value for the non-destructive estimation, although the mean R^2 is only 0.7775.

Figure 5 shows the boxplots of the five performance criteria for the 1000 iterations. This figure shows that boxplots are highly compressed and the amount of outlier data out of the box is very small. Figure 6 shows the actual value versus the mean estimated value of BrimA property (for the test set), i.e., the mean estimation for each sample after the 1000 iterations. As shown, the mean value set was able to estimate very accurately the actual measured values of the samples.
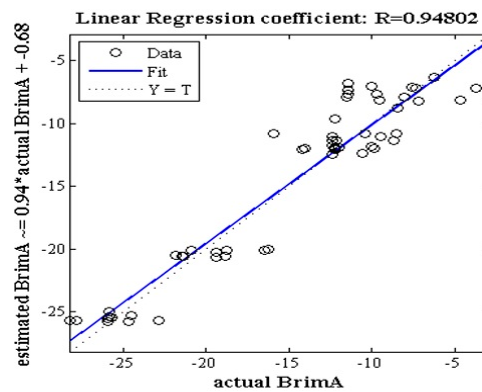
Figure 4. Regression analysis of the scatter plot between the estimated and the measured values of BrimA of the apples on the spectral range around the wavelength of 962 nm in the best training case.
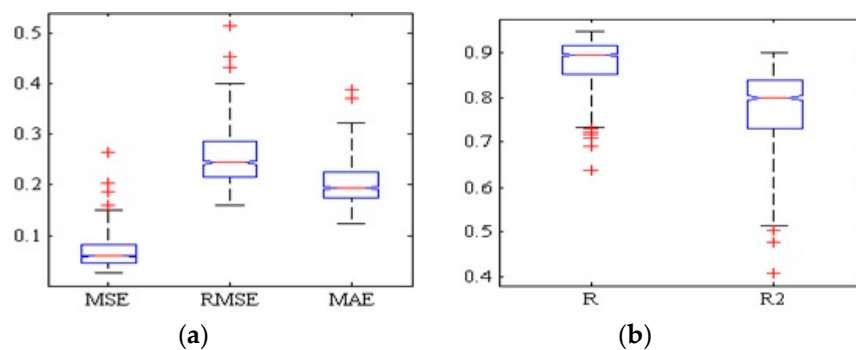

| (**a**) | (**b**) |

Figure 5. Boxplot of the evaluation criteria of the hybrid ANN–ABC method for estimating the BrimA value on spectral range around the wavelength of 962 nm at 1000 iterations. (**a**) Error measures: Mean Square Error (MSE), Root Mean Square Error (RMSE) and Mean Absolute Error (MAE). (**b**) Regression coefficient, R, and coefficient of determination, R^2.
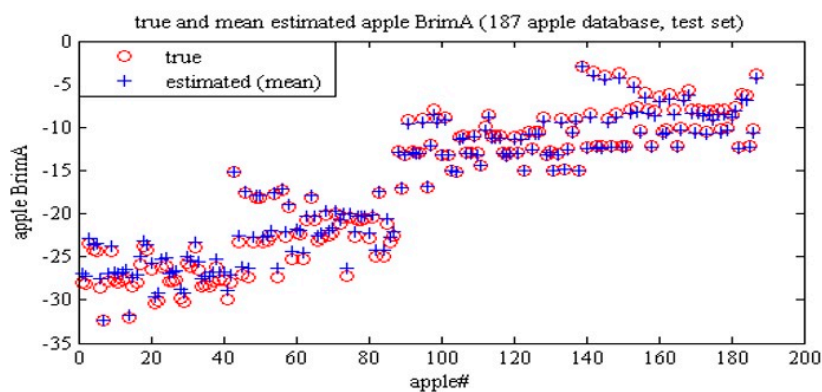

Figure 6. Measured values versus the mean estimated values of BrimA property for the test set. Each iteration contains 56 test samples; hence, there are 56,000 samples at 1000 iterations, and since there are only 187 samples, there are more than 299 iterations in each sample and their mean is calculated.

3.1.2. Estimation of the Firmness

The estimation of the firmness property using the hybrid ANN–ABC approach was also repeated 1000 times. In this case, spectral data around the wavelength of 875 nm was used. Table 4 presents the mean and SD values of the accuracy evaluation parameters.

Table 4. Mean and standard deviation of the performance evaluation parameters of the hybrid ANN–ABC method in estimating apple firmness on the spectral data around the wavelength range from 875 nm at 1000 iterations.

Criterion	MSE	RMSE	MAE	R	R^2
Mean	0.0422	0.2034	0.1503	0.7974	0.6377
Standard deviation	0.0118	0.0283	0.0187	0.0429	0.0674

Error measures: Mean Square Error (MSE), Root Mean Square Error (RMSE) and Mean Absolute Error (MAE). Regression coefficient, R, and coefficient of determination, R^2.

According to this table, the performance of the hybrid ANN–ABC method is unacceptable in the estimation of firmness using these spectral data, since the R^2 is relatively low. Figure 7 shows the regression analysis of the scatter plot between the estimated and the actual (measured) value of firmness of the apples for the best training execution. Figure 8 shows the boxplots of the performance criteria of estimation error and regression coefficients for the 1000 repetitions.
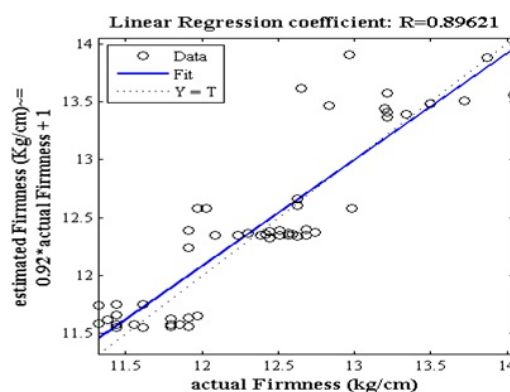

Figure 7. Regression analysis of the scatter plot between the estimated and the measured values of the apple firmness on the spectral range around the wavelength of 875 nm in the best training case.
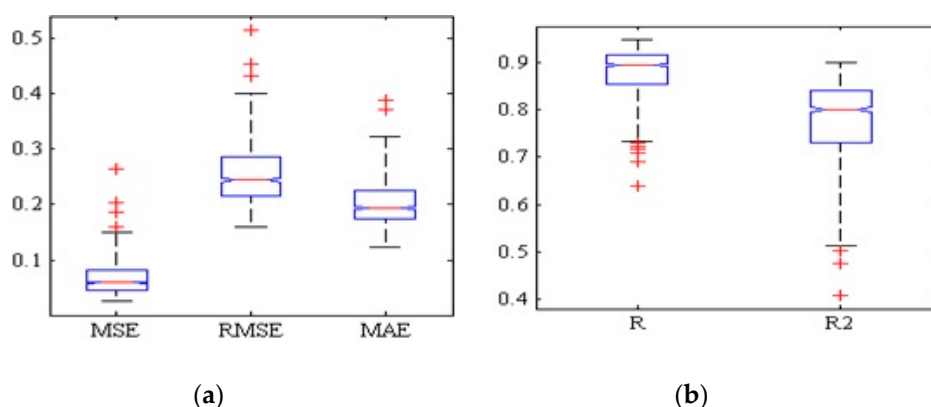

(**a**)　　　　　　　　　　　　　　　　　　　　　　　(**b**)

Figure 8. Boxplot of the evaluation criteria of the hybrid ANN–ABC method in estimating the value of firmness on the spectral range around the wavelength of 875 nm at 1000 iterations. (**a**) Error measures: Mean Square Error (MSE), Root Mean Square Error (RMSE) and Mean Absolute Error (MAE). (**b**) Regression coefficients and coefficient, R, of determination, R^2.

Figure 7 shows that, in the best training execution, this method is able to estimate the firmness with a coefficient of determination greater than 0.8. Figure 8 also indicates that more than half of the replicates are able to estimate the firmness with a coefficient of determination greater than 0.7, although there are some executions with a very poor result. Finally, Figure 9 shows that the mean value of the

firmness property for some apple samples is very close to the measured values, but there are some samples that produce a very high error.
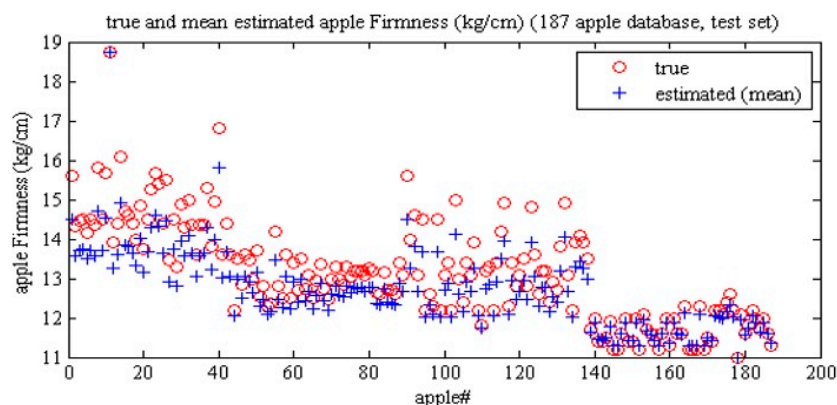

Figure 9. Measured values versus estimated values of the apple firmness for the test set. For each sample, the mean of around 299 estimations is calculated.

3.1.3. Estimation of the Acidity

Table 5 presents the mean and standard deviation of the accuracy measured in the estimation of acidity on the spectral range around 849 nm at 1000 iterations using the hybrid ANN–ABC method.

Table 5. Mean and standard deviation of the performance evaluation parameters of the hybrid ANN–ABC in estimating the acidity of spectral range around the wavelength of 849 nm at 1000 iterations.

Criterion	MSE	RMSE	MAE	R	R^2
Mean	0.0597	0.2431	0.1821	0.9053	0.8198
Standard deviation	0.0129	0.0240	0.0215	0.0173	0.0305

Error measures: Mean Square Error (MSE), Root Mean Square Error (RMSE) and Mean Absolute Error (MAE). Regression coefficient, R, and coefficient of determination, R^2.

Figure 10 contains the regression analysis of the scatter plot between the estimated and the measured value of acidity in the best training case. Figure 11 shows the boxplots of the accuracy criteria for the 1000 repetitions.
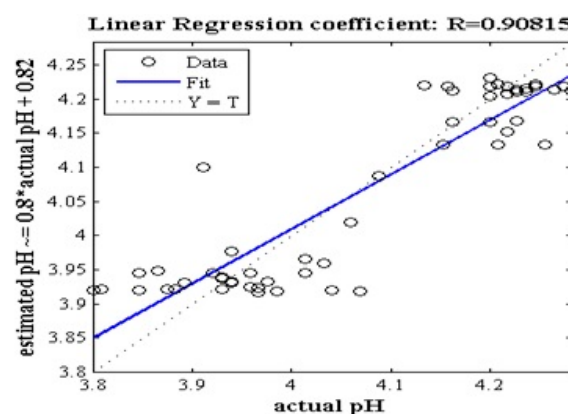

Figure 10. Regression analysis of the scatter plot between the estimated and the measured values of apple acidity on the spectral range around the wavelength of 849 nm in the best training case.

Table 5 and Figure 10 indicate that the coefficients of determination for both the mean of the 1000 iterations and the best training execution are greater than 0.8, which can be acceptable for the

non-destructive estimation. Figure 11 shows that the boxplots of all performance evaluation parameters of the hybrid ANN–ABC method are compact; hence, it can be argued that this method has close results in different iterations. Figure 12, which depicts the mean of the estimations, also shows that this method is able to achieve an accurate estimate of the acidity.
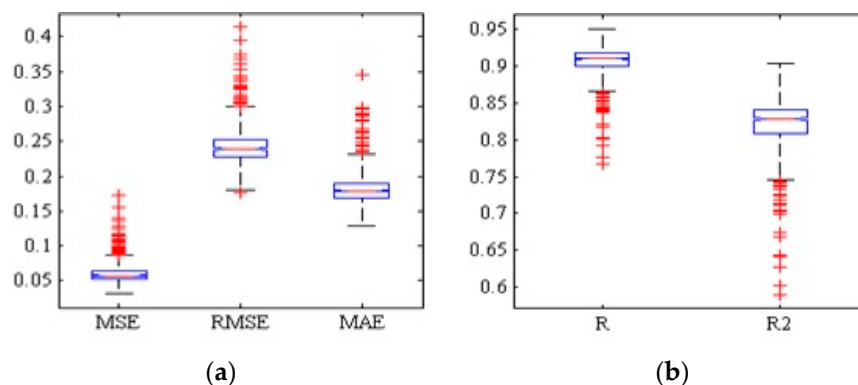

(**a**)   (**b**)

Figure 11. Boxplot of the evaluation criteria of the hybrid ANN–ABC method in estimating the acidity of spectral range around the wavelength of 849 nm at 1000 iterations. (**a**) Error measures: Mean Square Error (MSE), Root Mean Square Error (RMSE) and Mean Absolute Error (MAE). (**b**) Regression coefficient, R, and coefficient of determination, R^2.
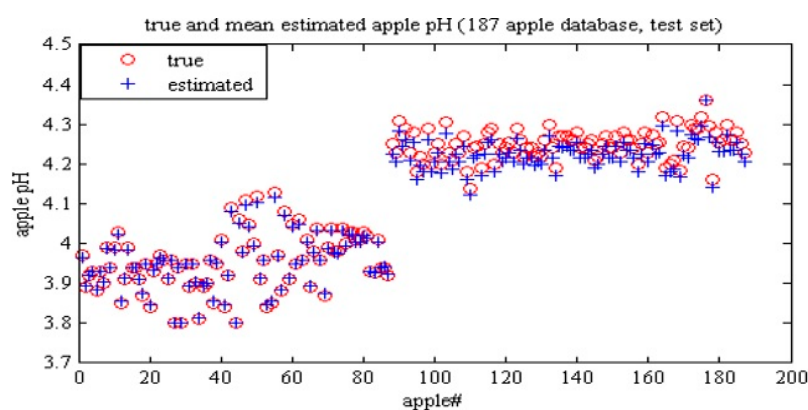

Figure 12. Measured values versus the estimated values of the acidity property for the test set. For each sample, the mean of around 299 estimations is calculated.

3.1.4. Estimation of the Starch Content

The experimental results for the estimation of the starch content of the apples are presented in Table 6 and Figures 13–15. In this case, the wavelength of 849 nm was used, and again the test was repeated 1000 iterations. As shown, the mean R^2 is greater than 0.94 for this method, and the R^2 in the best execution is greater than 0.97. In other words, the non-destructive starch estimation is very close to the measured values.

Table 6. Mean and standard deviation of the performance evaluation parameters of the hybrid ANN–ABC method in estimating starch content on the spectral range around the wavelength of 849 nm at 1000 iterations.

Criterion	MSE	RMSE	MAE	R	R^2
Mean	0.0190	0.1367	0.1047	0.9725	0.9458
Standard deviation	0.0053	0.0175	0.0135	0.0080	0.0155

Error measures: Mean Square Error (MSE), Root Mean Square Error (RMSE) and Mean Absolute Error (MAE). Regression coefficient, R, and coefficient of determination, R^2.
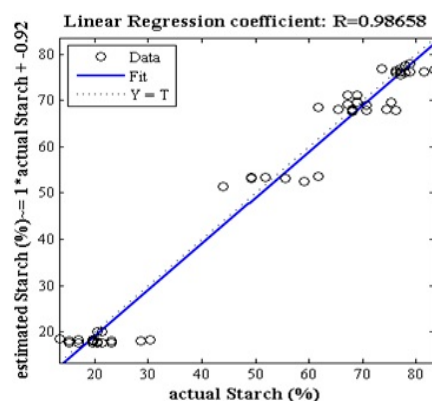
Figure 13. Regression analysis of the scatter plot between the estimated and the measured starch percentage of the apples on the spectral range around the wavelength of 849 nm at the best training execution.
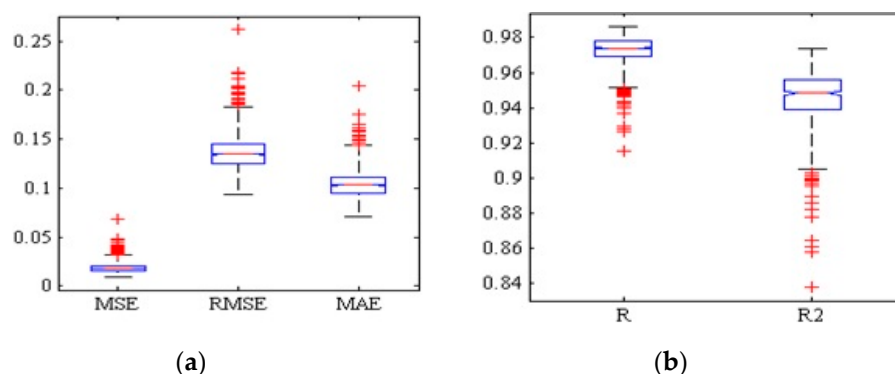

(**a**)　　　　　　　　　　　　　　　　　　　　(**b**)

Figure 14. Boxplot of the evaluation criteria of the hybrid ANN–ABC method in estimating starch content on the spectral range around the wavelength of 849 nm at 1000 iterations. (**a**) Error measures: Mean Square Error (MSE), Root Mean Square Error (RMSE) and Mean Absolute Error (MAE). (**b**) Regression coefficients, R, and coefficient of determination, R^2.
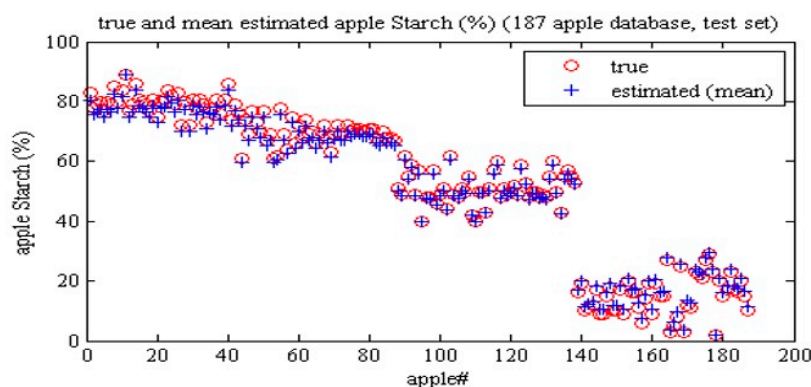

Figure 15. Measured values versus estimated values of the starch content of the apples for the test set. For each sample, the mean of 299 estimations is calculated.

3.2. Estimation of Physicochemical Properties Using the Most Effective Wavelengths

3.2.1. Estimation of BrimA Property

In this set of experiments, the estimation of the constituent properties of the apples is performed using only the most effective wavelengths selected in the hybrid approach ANN–PSO, described in Section 2. Tables 7 and 8 and Figure 16 show the effective wavelengths selected by this method for

the non-destructive estimation of BrimA, as well as the results of different performance evaluation criteria obtained in the estimation of BrimA using different numbers of effective wavelengths. Figure 16 presents a comparison of the measured values versus the estimated values of BrimA using the five most effective wavelengths selected by the hybrid ANN–PSO.

Table 7. Most effective wavelengths selected by the hybrid ANN–PSO for the estimation of BrimA.

Number of Wavelengths	Most Effective Wavelengths
2	959.3, 970.8
3	965.5, 958.1, 960.4
5	962.2, 969.0, 968.5, 960.8, 958.4
7	966.4, 966.1, 970.2, 965.2, 955.4, 957.8, 963.1
9	955.7, 959.3, 960.8, 961.9, 962.5, 963.7, 966.4, 969.0, 971.1

Table 8. Results of different performance evaluation criteria of the hybrid ANN–ABC method for the estimation of BrimA using different numbers of most effective wavelengths.

Num/Criterion	MSE	RMSE	MAE	R	R^2
2	13.44	3.67	2.85	0.891	0.794
3	25.72	5.07	3.92	0.840	0.706
5	11.44	3.38	2.42	0.910	0.828
7	20.26	4.50	3.29	0.830	0.689
9	19.58	4.42	3.61	0.839	0.704

Error measures: Mean Square Error (MSE), Root Mean Square Error (RMSE) and Mean Absolute Error (MAE). Regression coefficient, R, and coefficient of determination, R^2.
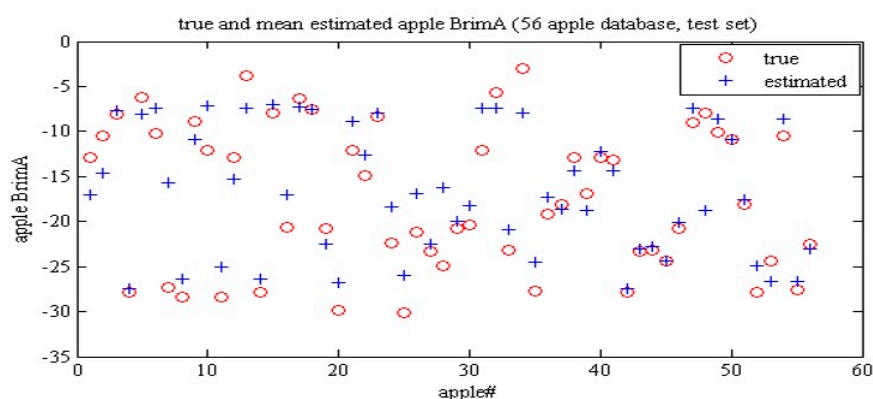

Figure 16. Measured values versus estimated values of BrimA property for the test set, using the five most effective wavelengths selected by the hybrid ANN–PSO algorithm.

The highest value of R^2 is 0.828 for the non-destructive estimation of the value of BrimA, and it is related to the input data by the hybrid ANN–ABC method with five wavelengths.

3.2.2. Estimation of the Firmness

Tables 9 and 10 and Figure 17 present the results of the non-destructive estimation of firmness using the most effective wavelengths. According to Table 10, the hybrid ANN–ABC method is not able to estimate correctly the firmness of the apples in four of the five cases. Only the estimation using nine wavelengths achieves an R^2 of 0.738, which is still not a very high value. This problem is consistent with the results obtained using all the spectral information, where it was observed that the firmness of the apples could not be estimated accurately.
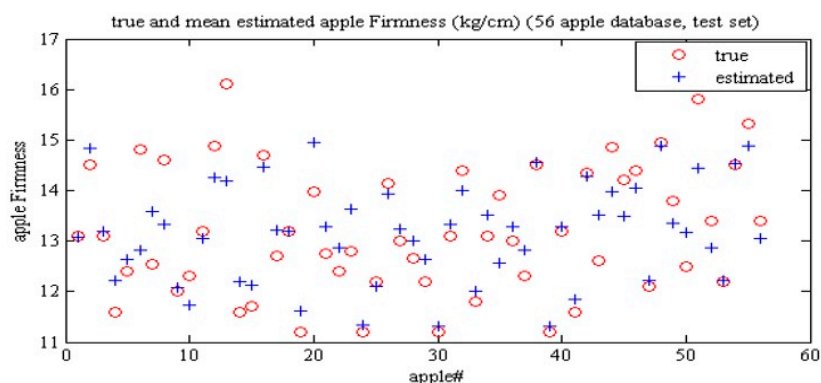
Table 9. Most effective wavelengths selected by the hybrid ANN–PSO method for the estimation of the firmness of the apples.

Number of Wavelengths	Most Effective Wavelengths
2	882.1, 869.4
3	870.3, 872.4, 882.1
5	872.4, 869.1, 872.7, 876.5, 882.7
7	875.3, 870.9 880.1, 868.3, 879.5, 874.5, 872.4
9	870.6, 878.3, 884.8, 874.5, 873. 0, 874.8, 880.4, 876.2, 868.6

Table 10. Results of different performance evaluation criteria of the hybrid ANN–ABC method for the non-destructive estimation of firmness using different numbers of most effective wavelengths.

Num/Criterion	MSE	RMSE	MAE	R	R^2
2	0.577	0.759	0.548	0.765	0.585
3	0.649	0.806	0.592	0.760	0.577
5	0.609	0.781	0.633	0.711	0.506
7	0.933	0.966	0.668	0.699	0.489
9	0.416	0.645	0.472	0.859	0.738

Error measures: Mean Square Error (MSE), Root Mean Square Error (RMSE) and Mean Absolute Error (MAE). Regression coefficient, R, and coefficient of determination, R^2.

Figure 17. Measured values versus estimated values of the apple firmness for the test set, using the nine most effective wavelengths selected by the hybrid ANN–PSO algorithm.

3.2.3. Estimation of the Acidity

The results of the proposed non-destructive estimation of acidity are presented in Tables 11 and 12 and in Figure 18, using in this case the seven most effective wavelengths.

As shown, the highest R^2 in the estimation of acidity is related to the case that uses seven wavelengths as the input of the hybrid ANN–ABC method. The value of R^2 is greater than 0.9 in this case, which can be considered a very accurate estimation.
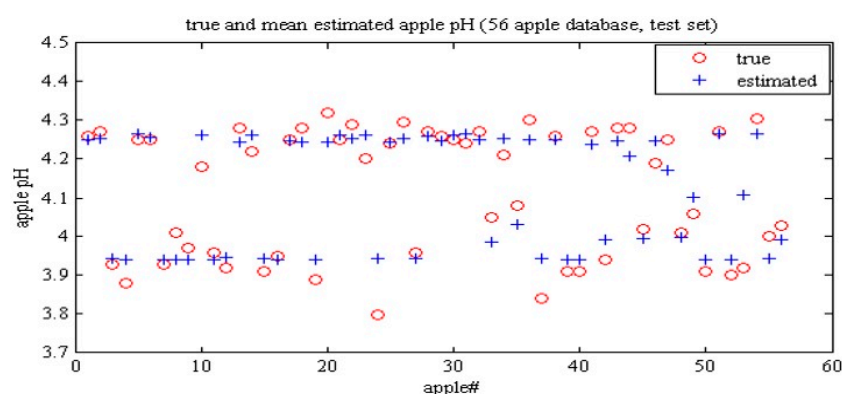
Table 11. Most effective wavelengths selected by the hybrid ANN–PSO method for the estimation of the acidity.

Number of Wavelengths	Most Effective Wavelengths
2	846.1, 852.3
3	843.4, 845.2, 853.8
5	851.4, 841.9, 855.0, 844.0, 852.0
7	850.8, 846.7, 852.6, 841.4, 844.9, 855.8, 850.5
9	846.1, 850.8, 848.2, 855.0, 852.9, 848.7, 852.0, 855.1, 868.5

Table 12. Results of different performance evaluation criteria of the hybrid ANN–ABC method for the non-destructive estimation of acidity using different numbers of most effective wavelengths.

Num/Criterion	MSE	RMSE	MAE	R	R^2
2	0.0040	0.0635	0.0471	0.9095	0.8272
3	0.0027	0.0518	0.0399	0.9405	0.8845
5	0.0036	0.0600	0.0430	0.9235	0.8529
7	0.0027	0.0522	0.0400	0.9487	0.9001
9	0.0044	0.0662	0.0500	0.9096	0.8273

Error measures: Mean Square Error (MSE), Root Mean Square Error (RMSE) and Mean Absolute Error (MAE). Regression coefficient, R, and coefficient of determination, R^2.

Figure 18. Measured values versus estimated values of the apple acidity for the test set, using the seven most effective wavelengths selected by the hybrid ANN–PSO.

3.2.4. Estimation of the Starch Content

Table 13 presents the most effective wavelengths selected by the hybrid ANN–PSO method for the non-destructive estimation of the starch content of the apples. Table 14 shows the results of the performance criteria of the hybrid ANN–ABC using different numbers of effective properties. The comparison between the measured values and the estimated values of starch content using the five wavelengths selected by the hybrid ANN–PSO method are depicted in Figure 19.

Table 13. Most effective wavelengths selected by the hybrid ANN–PSO method for the estimation of the starch content.

Number of Wavelengths	Most Effective Wavelengths
2	849.3, 854.4
3	851.1, 853.8, 849.0
5	851.4, 845.2, 842.2, 844.9, 852.9
7	841.6, 844.0, 851.7, 848.4, 845.8, 846.4, 850.8
9	846.0, 852.9, 848.4, 841.4, 852.6, 849.9, 851.1, 841.1, 841.6

Table 14. Results of different performance evaluation criteria of the hybrid ANN–ABC method for the non-destructive estimation of starch content using different numbers of most effective wavelengths.

Num/Criterion	MSE	RMSE	MAE	R	R^2
2	75.42	8.68	6.18	0.943	0.889
3	87.97	9.38	7.24	0.945	0.893
5	49.84	7.06	5.40	0.961	0.923
7	119.57	10.93	7.97	0.883	0.780
9	58.85	7.67	6.28	0.958	0.918

Error measures: Mean Square Error (MSE), Root Mean Square Error (RMSE) and Mean Absolute Error (MAE). Regression coefficient, R, and coefficient of determination, R^2.
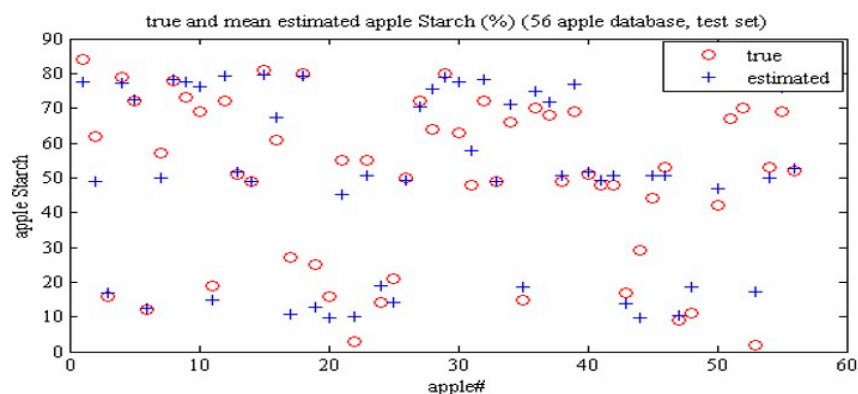
Figure 19. Measured values versus estimated values of starch content of the apples for the test set, using the five most effective wavelengths selected by the hybrid ANN–PSO method.

As shown in Table 14, the highest R^2 is related to the case that uses five wavelengths to estimate the amount of starch, and it is equal to 0.923, which is again a very good result.

3.3. Comparison of the Proposed Method with Other Research Works

3.3.1. Non-Destructive Estimation of the Firmness

This subsection compares the accuracy of the proposed method with the results reported by other authors that also estimate the firmness of different fruits using spectral information. Three works have been found in the literature, proposed by Bizzani et al. [20], Uwadaira et al. [35] and Huang et al. [36]. Table 15 describes the main features of these works and the obtained values of the coefficient of determination, R^2.

Table 15. Comparison of the proposed method with other previous studies for the non-destructive estimation of firmness based on the coefficient of determination, R^2.

Researchers	Type of Fruit	Method (Spectrum Unit: nm)	R^2
Proposed method	Apple	868 to 884 nm	0.803
Bizzani et al. [20]	Orange	1000 to 2500 nm	0.92
Uwadaira et al. [35]	Peach	500 to 1000 nm	0.8
Huang et al. [36]	Tomato	300 to 550 nm	0.894

Coefficient of determination, R^2.

As shown in Table 15, the highest R^2 of this property is achieved in the spectral range between 1000 and 2500 nm. Since the amount of tissue firmness is directly related to the amount of fruit juice, it is possible to perform the non-destructive prediction of the amount of tissue firmness by the opposite action of the NIR spectrum. According to Abbott's research, there is an absorption peak between spectra of 1400 nm and 1500 nm due to the presence of water in the fruit tissue [37]. This justifies that the R^2 obtained in our work is not very high, since the spectral range is outside of the ideal range.

3.3.2. Non-Destructive Estimation of the Acidity

In the case of the acidity, the most related works are due to Huang et al. [36], Cavaco et al. [38] and Cayuela [23]. Table 16 shows the comparison of the proposed method and these works.

As shown in Table 16, the R^2 of the proposed method is higher than those of the other methods for the non-destructive estimation of the acidity, but still, it is not an acceptable value. The reasons for this case may be similar to those for the titratable acidity.

Table 16. Comparison of the proposed method with other previous studies for the non-destructive estimation of the acidity based on the coefficient of determination, R^2.

Researchers	Type of Fruit	Method (Spectrum Unit: nm)	R^2
Proposed method	Apple	841 to 855 nm	0.825
Huang et al. [36]	Tomato	400 to 1100 nm	0.64
Cavaco et al. [38]	Orange	733 to 1000 nm	0.52
Cayuela [23]	Orange	578 to 1850 nm	0.45

Coefficient of determination, R^2.

3.3.3. Non-Destructive Estimation of the Starch Content

Concerning the estimation of the starch content in fruits, only two previous papers were found, due to Jiang and Lu [39] and Ignat et al. [40]. Table 17 compares the results reported in these works with the proposed method.

Table 17. Comparison of the proposed method with other previous studies for the non-destructive estimation of the starch content based on the coefficient of determination, R^2.

Researchers	Type of Fruit	Method (Spectrum Unit: nm)	R^2
Propose method	Apple	841 to 855 nm	0.97
Jiang and Lu [39]	Corn	1100 to 2500 nm	0.99
Ignat et al. [40]	Apple	340 to 1014 nm	0.91

Coefficient of determination, R^2.

As can be observed in Table 17, the results of all these studies are acceptable because they have high coefficients of determination. The major spectral regions of starch aggregation are the spectral region from 800 to 1000 nm, and the wavelengths greater than 1700 nm [37]. This table shows that the spectral domain has an acceptable range in all studies and, thus, the results are acceptable.

4. Conclusions

In this study, a new non-destructive method based on the hybrid Artificial Neural Networks–Particle Swarm Optimization (ANN–PSO) algorithm and on the hybrid Artificial Neural Networks-Artificial Bee Colony (ANN–ABC) algorithm has been proposed to estimate some mechanical and physicochemical properties of Red Delicious apples, namely BrimA, firmness, acidity and starch content, using spectral data in the range between 400 and 1000 nm.

Four main conclusions can be drawn from the experimental results. First, the selection of the appropriate spectral ranges is essential to increase the estimation accuracy of the spectral data-based methods. Second, the predicted starch content of the Red Delicious apple was very close to actual measured values in the spectral range from 400 to 1000 nm. Third, the results obtained with the use of the most effective wavelengths produced coefficients of determination lower than those obtained using a wide range of spectral properties, but the difference was not significant. Fourth, the selection of the most appropriate spectral range, and the use of effective machine learning techniques guaranteed high performance of the proposed method in the present study.

For future works, we suggest developing a non-destructive method to estimate the ripeness of Red Delicious apples. The spectral measurements of the above-mentioned physicochemical properties will be used as features to determine the ripening state of the fruits. Artificial Neural Networks (ANN) and deep learning techniques could be an interesting way to achieve this goal.

Author Contributions: Conceptualization, Y.A.-G. and S.S.; methodology, Y.A.-G., S.S., B.B., G.G.-M. and J.L.H.-H.; software, S.S.; validation, Y.A.-G., S.S. and B.B.; formal analysis, S.S., B.B. and G.G.-M.; investigation, Y.A.-G., S.S., B.B., G.G.-M., J.L.H.-H. and J.M.M.-M.; resources, Y.A.-G. and S.S.; writing—original draft preparation, Y.A.-G. and S.S.; writing—review and editing, B.B., G.G.-M. and J.L.H.-H.; supervision, Y.A.-G.; project administration,

References

1. Bexiga, F.; Rodrigues, D.; Guerra, R.; Brázio, A.; Balegas, T.; Cavaco, A.M.; Antunes, M.D.; de Oliveira, J.V. A TSS classification study of 'Rocha'pear (Pyrus communis L.) based on non-invasive visible/near infra-red reflectance spectra. *Postharvest Biol. Technol.* **2017**, *132*, 23–30. [CrossRef]

2. Opara, U.L.; Pathare, P.B. Bruise damage measurement and analysis of fresh horticultural produce-A review. *Postharvest Biol. Technol.* **2014**, *91*, 9–24. [CrossRef]

3. Arendse, E.; Fawole, O.A.; Magwaza, L.S.; Opara, U.L. Non-destructive prediction of internal and external quality attributes of fruit with thick rind: A review. *J. Food Eng.* **2018**, *217*, 11–23. [CrossRef]

4. Chen, L.; Opara, U.L. Approaches to analysis and modeling texture in fresh and processed foods—A review. *J. Food Eng.* **2013**, 497–507. [CrossRef]

5. Chen, L.; Opara, U.L. Texture measurement approaches in fresh and processed foods—A review. *Food Res. Int.* **2013**, 823–835. [CrossRef]

6. Magwaza, L.S.; Opara, U.L. Analytical methods for determination of sugars and sweetness of horticultural products—A review. *Sci. Hortic. (Amsterdam)* **2015**, 179–192. [CrossRef]

7. Nicolaï, B.M.; Beullens, K.; Bobelyn, E.; Peirs, A.; Saeys, W.; Theron, K.I.; Lammertyn, J. Nondestructive measurement of fruit and vegetable quality by means of NIR spectroscopy: A review. *Postharvest Biol. Technol.* **2007**, 99–118. [CrossRef]

8. Beghi, R.; Buratti, S.; Giovenzana, V.; Benedetti, S.; Guidetti, R. Electronic nose and visible-near infrared spectroscopy in fruit and vegetable monitoring. *Rev. Anal. Chem.* **2017**, *36*. [CrossRef]

9. Cozzolino, D. An overview of the use of infrared spectroscopy and chemometrics in authenticity and traceability of cereals. *Food Res. Int.* **2014**, *60*, 262–265. [CrossRef]

10. Lohumi, S.; Lee, S.; Lee, H.; Cho, B.K. A review of vibrational spectroscopic techniques for the detection of food authenticity and adulteration. *Trends Food Sci. Technol.* **2015**, *46*, 85–98. [CrossRef]

11. Daniel, C. The role of visible and infrared spectroscopy combined with chemometrics to measure phenolic compounds in grape and wine samples. *Molecules* **2015**, *20*, 726–737. [CrossRef]

12. Roychoudhury, P.; Harvey, L.M.; McNeil, B. The potential of mid infrared spectroscopy (MIRS) for real time bioprocess monitoring. *Anal. Chim. Acta* **2006**, 159–166. [CrossRef] [PubMed]

13. Menesatti, P.; Zanella, A.; D'Andrea, S.; Costa, C.; Paglia, G.; Pallottino, F. Supervised multivariate analysis of hyper-spectral NIR images to evaluate the starch index of apples. *Food Bioprocess Technol.* **2009**, *2*, 308–314. [CrossRef]

14. De Carvalho Polari Souto, U.T.; Barbosa, M.F.; Dantas, H.V.; de Pontes, A.S.; da Silva Lyra, W.; Diniz, P.H.G.D.; de Araújo, M.C.U.; da Silva, E.C. Identification of adulteration in ground roasted coffees using UV-Vis spectroscopy and SPA-LDA. *LWT Food Sci. Technol.* **2015**, *63*, 1037–1041.

15. Aprea, E.; Biasioli, F.; Sani, G.; Cantini, C.; Märk, T.D.; Gasperi, F. Proton transfer reaction-mass spectrometry (PTR-MS) headspace analysis for rapid detection of oxidative alteration of olive oil. *J. Agric. Food Chem.* **2006**, *54*, 7635–7640. [CrossRef] [PubMed]

16. Ciesa, F.; Dalla Via, J.; Wisthaler, A.; Zanella, A.; Guerra, W.; Mikoviny, T.; Märk, T.D.; Oberhuber, M. Discrimination of four different postharvest treatments of "Red Delicious" apples based on their volatile organic compound (VOC) emissions during shelf-life measured by proton transfer reaction mass spectrometry (PTR-MS). *Postharvest Biol. Technol.* **2013**, *86*, 329–336. [CrossRef]

17. Cozzolino, D. Near infrared spectroscopy in natural products analysis. *Planta Med.* **2009**, *75*, 746–756. [CrossRef]

18. Moscetti, R.; Haff, R.P.; Monarca, D.; Cecchini, M.; Massantini, R. Near-infrared spectroscopy for detection of hailstorm damage on olive fruit. *Postharvest Biol. Technol.* **2016**, *120*, 204–212. [CrossRef]

19. Figueiredo Neto, A.; Cárdenas Olivier, N.; Rabelo Cordeiro, E.; Pequeno de Oliveira, H. Determination of mango ripening degree by electrical impedance spectroscopy. *Comput. Electron. Agric.* **2017**, *143*, 222–226. [CrossRef]

20. Bizzani, M.; Flores, D.W.M.; Colnago, L.A.; Ferreira, M.D. Non-invasive spectroscopic methods to estimate orange firmness, peel thickness, and total pectin content. *Microchem. J.* **2017**, *133*, 168–174. [CrossRef]

21. Xie, L.; Ye, X.; Liu, D.; Ying, Y. Prediction of titratable acidity, malic acid, and citric acid in bayberry fruit by near-infrared spectroscopy. *Food Res. Int.* **2011**, *44*, 2198–2204. [CrossRef]

22. Viscarra Rossel, R.A. ParLeS: Software for chemometric analysis of spectroscopic data. *Chemom. Intell. Lab. Syst.* **2008**, *90*, 72–83. [CrossRef]

23. Cayuela, J.A. Vis/NIR soluble solids prediction in intact oranges (Citrus sinensis L.) cv. Valencia Late by reflectance. *Postharvest Biol. Technol.* **2008**, *47*, 75–80. [CrossRef]

24. Martínez-Valdivieso, D.; Font, R.; Blanco-Díaz, M.T.; Moreno-Rojas, J.M.; Gómez, P.; Alonso-Moraga, Á.; Del Río-Celestino, M. Application of near-infrared reflectance spectroscopy for predicting carotenoid content in summer squash fruit. *Comput. Electron. Agric.* **2014**, *108*, 71–79. [CrossRef]

25. Xiaobo, Z.; Jiewen, Z.; Povey, M.J.W.; Holmes, M.; Hanpin, M. Variables selection methods in near-infrared spectroscopy. *Anal. Chim. Acta* **2010**, *667*, 14–32. [CrossRef]

26. Jordan, R.B.; Seelye, R.J.; McGlone, V.A. A sensory-based alternative to brix/acid ratio. *Food Technol.* **2001**, *55*, 36–44.

27. Ncama, K.; Opara, U.L.; Tesfay, S.Z.; Fawole, O.A.; Magwaza, L.S. Application of Vis/NIR spectroscopy for predicting sweetness and flavour parameters of 'Valencia' orange (Citrus sinensis) and 'Star Ruby' grapefruit (Citrus x paradisi Macfad). *J. Food Eng.* **2017**, *193*, 86–94. [CrossRef]

28. Wongkhot, A.; Rattanapanone, N.; Chanasut, U. Brima, total acidity and total soluble solids correlate to total carotenoid content as indicators of the ripening process of six thai mango fruit cultivars. *Chiang Mai Univ. J. Nat. Sci.* **2012**, *11*, 97–103.

29. De Belie, N.; Schotte, S.; Lammertyn, J.; Nicolai, B.; De Baerdemaeker, J. Firmness changes of pear fruit before and after harvest with the acoustic impulse response technique. *J. Agric. Eng. Res.* **2000**.

30. Gao, H.; Cai, J.; Han, W.; Huai, H.; Chen, Y.; Wei, C. Comparison of starches isolated from three different Trapa species. *Food Hydrocoll.* **2014**, *37*, 174–181. [CrossRef]

31. Kennedy, J.; Eberhart, R. Particle Swarm Optmization. In Proceedings of the IEEE International Conference on Neural Networks, Perth, Australia, 27 November–1 December 1995.

32. Hussein, W.A.; Sahran, S.; Abdullah, S.N.H.S. A fast scheme for multilevel thresholding based on a modified bees algorithm. *Knowledge-Based Syst.* **2016**, *101*, 114–134. [CrossRef]

33. Sabzi, S.; Javadikia, P.; Rabani, H.; Adelkhani, A. Mass modeling of Bam orange with ANFIS and SPSS methods for using in machine vision. *Meas. J. Int. Meas. Confed.* **2013**, *46*, 3333–3341. [CrossRef]

34. Sabzi, S.; Arribas, J.I. A visible-range computer-vision system for automated, non-intrusive assessment of the pH value in Thomson oranges. *Comput. Ind.* **2018**, *99*, 69–82. [CrossRef]

35. Uwadaira, Y.; Sekiyama, Y.; Ikehata, A. An examination of the principle of non-destructive flesh firmness measurement of peach fruit by using VIS-NIR spectroscopy. *Heliyon* **2018**, *4*, e00531. [CrossRef] [PubMed]

36. Huang, Y.; Lu, R.; Chen, K. Assessment of tomato soluble solids content and pH by spatially-resolved and conventional Vis/NIR spectroscopy. *J. Food Eng.* **2018**, *236*, 19–28. [CrossRef]

37. Abbott, J.A. Quality measurement of fruits and vegetables. *Postharvest Biol. Technol.* **1999**, *15*, 207–225. [CrossRef]

38. Cavaco, A.M.; Pires, R.; Antunes, M.D.; Panagopoulos, T.; Brázio, A.; Afonso, A.M.; Silva, L.; Lucas, M.R.; Cadeiras, B.; Cruz, S.P.; et al. Validation of short wave near infrared calibration models for the quality and ripening of 'Newhall' orange on tree across years and orchards. *Postharvest Biol. Technol.* **2018**, *141*, 86–97. [CrossRef]

39. Jiang, H.; Lu, J. Using an optimal CC-PLSR-RBFNN model and NIR spectroscopy for the starch content determination in corn. *Spectrochim. Acta Part A Mol. Biomol. Spectrosc.* **2018**, *196*, 131–140. [CrossRef]
40. Ignat, T.; Lurie, S.; Nyasordzi, J.; Ostrovsky, V.; Egozi, H.; Hoffman, A.; Friedman, H.; Weksler, A.; Schmilovitch, Z. Forecast of Apple Internal Quality Indices at Harvest and During Storage by VIS-NIR Spectroscopy. *Food Bioprocess Technol.* **2014**, *7*, 2951–2961. [CrossRef]